# Journal of Materials Chemistry C

Accepted Manuscript


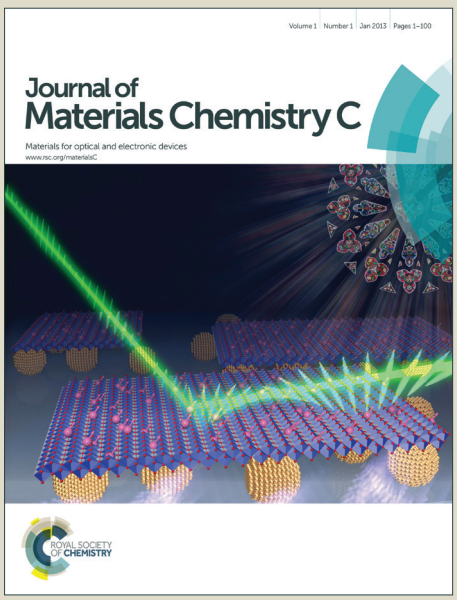





ROYAL SOCIETY OF CHEMISTRY

www.rsc.org/materialsC

Cite this: DOI: 10.1039/c0xx00000x

www.rsc.org/xxxxxx

ARTICLE TYPE

# Structure and luminescent properties of a novel yellow super long lasting phosphate phosphor $Ca_6BaP_4O_{17}:Eu^{2+},Ho^{3+}$

**Haijie Guo, Wenbo Chen, Wei Zeng, Gen Li, Yuhua Wang*, Yanyan Li, Yang Li, and Xin Ding**

***Received (in XXX, XXX) Xth XXXXXXXXX 20XX, Accepted Xth XXXXXXXXX 20XX***

**DOI: 10.1039/b000000x**

A novel yellow emitting long lasting phosphate phosphor $Ca_6BaP_4O_{17}:Eu^{2+},Ho^{3+}$ is developed. The incorporation of $Ho^{3+}$ ions, which act as trap centers, largely extends the thermoluminescence characteristics and evidently enhances the persistent luminescence behavior of the phosphor. Both fluorescence and phosphorescence spectra of $Ca_6BaP_4O_{17}:0.02Eu^{2+},0.015Ho^{3+}$ reveal only one asymmetric broad emission band located at 553 nm, ascribed to the 5d-4f transitions of $Eu^{2+}$ ions in two different $Ca^{2+}$ sites. After 15 min excitation, the initial long lasting phosphoresce (LLP) intensity of $Ca_6BaP_4O_{17}:0.02Eu^{2+},0.015Ho^{3+}$ can reach about 0.13 cd/m $^2$ and its LLP can last more than 47 h above the recognizable intensity level (0.32 mcd/m $^2$), a phenomenon that is infrequent and excellent. Furthermore, the direct bandgap of about 4.081 eV for $Ca_6BaP_4O_{17}$ provides suitable bandgap for $Eu^{2+}$ and $Ho^{3+}$ ions. The results indicate that the phosphor has potential to become a novel commercial LLP phosphor used in the field of emergency lighting and display. Detailed processes and possible mechanism are studied and discussed.

## 1. Introduction

Long-lasting phosphorescence (LLP) phosphors are a special kind of energy-storing materials, which could store the energy and then release it in the form of persistent visible light usually in room temperature.[1] In recent years, persistent luminescence materials have attracted much attention worldwide due to their commercial applications in the field of emergent lighting and display and their potential applications in such fields as high-energy irradiation dosimeters, rewritable three-dimensional optical memory materials, persistent photocatalytic, medical diagnostics and vivo bio-imaging, *etc*.[2,3,4,5]

Since Matsuzawa *et al.* discovered $SrAl_2O_4:Eu^{2+},Dy^{3+}$ in the middle of the1990s,[6] extensive research on different afterglow materials has been conducted aimed at tuning their emission color, prolonging their persistent luminescence and providing fundamental understanding of the afterglow mechanism.[7] Different synthesis methods, various co-dopants, and fluxes were investigated.[8,9,10] Those studies have brought new interesting afterglow phosphors emitting mostly in the blue-green spectral range. Until now, the most efficient afterglow phosphors are blue-green emitting $Eu^{2+}$ ions doped aluminates and silicates, e.g. $Sr_2MgSi_2O_7:Eu^{2+},Dy^{3+}$ (blue, >10 h),[11] $Sr_4Al_{14}O_{25}:Eu^{2+},Dy^{3+}$ (blue, >15 h),[12] $SrAl_2O_4:Eu^{2+},Dy^{3+}$ (green, >24 h).[13] Yellow and red emitting afterglow phosphors are in great scarcity, e.g. $Sr_3SiO_5:Eu^{2+},Dy^{3+}$ (yellow, >6 h),[14] $Y_2O_2S:Eu^{3+},Ti^{4+},Mg^{2+}$ (orange-red, >5 h),[15] $Ca_2Si_5N_8:Eu^{2+},Tm^{3+}$ (red, >1 h),[16] and $Mg_2SiO_4:Dy^{3+},Mn^{2+}$ (red, >17 min),[17] and $Mg_2SiO_4:Dy^{3+},Mn^{2+}$ (red, >17 min),[17] but most of them have poor chemical stability, low luminous intensity, short duration time and the preparation condition of nitrides is rigorous compared with other commercial persistent phosphors. Besides, yellow-emitting match the maximum sensitivity of human vision. Thus, the development of efficient yellow emitting afterglow phosphors is still an ongoing challenge.[18]

In order to achieve a yellow emitting long-persistent phosphor, we tentatively aimed at a calcium barium phosphate, $Ca_6BaP_4O_{17}$. Although there is no reports on the LLP phenomenon of $Ca_6BaP_4O_{17}$ to the best of our knowledge, phosphate compounds have excellent thermal stability and stabilization of ionic charge in the lattice, compared to other oxide phosphors.[19] Moreover, rare earth activated phosphate phosphors have been proven to be efficient phosphors. Recently, Naoyuki Komuro *et al.* discovered the phase of $Ca_6BaP_4O_{17}$ with a monoclinic structure in space group C2/m and reported $Ca_6BaP_4O_{17}:Eu^{2+}$ phosphor with strong yellow emission and a new blue-green phosphor $Ca_6BaP_4O_{17}:Ce^{3+}$ for light emitting diodes.[20,21] In this article, $Ho^{3+}$ ions were considered and introduced as trap centers into $Ca_6BaP_4O_{17}:Eu^{2+}$ host due to $Ho^{3+}$ ions can provide appropriate traps under Dorenbos' theory.[22] On the basis of these, we successfully synthesized a novel yellow emitting long lasting phosphor $Ca_6BaP_4O_{17}:Eu^{2+},Ho^{3+}$ with excellent afterglow properties via a traditional solid-state reaction method. We also investigated the defect properties of $Ca_6BaP_4O_{17}:Eu^{2+},Ho^{3+}$ by means of decay curves and thermoluminescence (TL) spectra, which revealed that the $Ho^{3+}$ ions incorporated into the phosphor dramatically increased the afterglow performance via promoting defect levels in the phosphor.

## 2. Experimental

In this work, the investigated samples $Ca_6BaP_4O_{17}$:0.02$Eu^{2+}$,$yHo^{3+}$ ($y$=0, 0.005, 0.01, 0.015, 0.02 and 0.03, which are denoted as S1-S6, respectively) were synthesized through the conventional high-temperature solid-state method with $CaCO_3$ (A.R.), $BaCO_3$ (99.99%), $NH_4H_2PO_4$ (A.R.), $Ho_2O_3$ (99.99%) and $Eu_2O_3$ (99.99%) as raw materials. The stoichiometric amounts of the corresponding starting materials were homogeneously mixed and thoroughly ground in an agate mortar by adding an appropriate amount of ethanol, and ground for 30 min, and subsequently the mixture were placed into an alumina crucibles and sintered at 1280 °C for 10 h under reducing atmosphere ($N_2$:$H_2$ = 95:5) in an electric tube furnace. After calcining, the samples were cooled to room temperature in the furnace and ground again for subsequent use.

All the phase structures of samples were characterized by powder X-ray diffraction (XRD) using a Rigaku diffractometer with Nifiltered Cu Kα radiation at scanning steps of 0.02° in the 2θ range from 10° to 80°. The excitation and emission spectra were measured by a FLS-920T fluorescence spectrophotometer with Xe 900 (450 W xenon arc lamp) as the excitation source. The scanning step was 1 nm. Afterglow decay curve measurements were measured with a PR305 long afterglow instrument after the samples were irradiated with ultraviolet light for 15 min. The TL curves were measured with a FJ-427A TL meter (Beijing Nuclear Instrument Factory) with a heating rate of 1 K $s^{-1}$ in the temperature range from 20 to 400 °C. Before measurement, 0.0001 g samples pressed in pellets were exposed to radiation for 2 min by UV lights. All measurements were carried out at room temperature except for the TL curves.

The calculations of the electronic structure for $Ca_6BaP_4O_{13}$ were carried out with density functional theory and performed with CASTEP code. The local-density approximations based on density functional theory were chosen for the theoretical basis of the density function.

## 3. Results and discussion

### 3.1. XRD patterns and Rietveld refinement

The experimental values, calculated values, peak positions and difference of Rietveld refinement XRD patterns of $Ca_6BaP_4O_{17}$ host are shown in Fig. 1a, the $Ca_6BaP_4O_{17}$ sample was refined using the Maud refinement program by the Rietveld method.[23,24] The residual factors are $Rwp$ = 10.68%, and $Rp$ = 8.91%, indicating that there fined results were reliable. Besides, the unit cell parameters are $a$ = 12.3052 (2) Å, $b$ = 7.1040 (1) Å, $c$ = 11.7167 (2) Å, $\beta$ = 134.4407 (6)°. It can be seen that all the observed peaks satisfy well with the simulated XRD patterns. The final refinement results indicate that the powder sample is crystallized in $Ca_6BaP_4O_{17}$ structure with space group C2/m and provides two different sites for $Ca^{2+}$ ions as shown in the inset of Fig. 1a and a single Ba site. Based on the consideration of effective ionic radii with different coordination numbers (CN), the doping rare-earth ions, $Eu^{2+}$ ($r$ = 1.20 Å, CN = 7; $r$ = 1.25 Å, CN = 8) and $Ho^{3+}$ ( $r$ = 1.015 Å, CN = 8) are proposed to occupy two $Ca^{2+}$ ($r$ = 1.06 Å, CN = 7; $r$ = 1.12 Å, CN = 8) sites rather than $Ba^{2+}$ ($r$ = 1.61 Å, CN = 12) sites in the $Ca_6BaP_4O_{17}$ host lattice. Fig. 1b shows the typical XRD patterns of samples (S1-S6). As can be seen, no extra phase is observed, indicating that the samples obtained have a single phase and that doping with a small amount of $Eu^{2+}$ ions and $Ho^{3+}$ ions will not induce any impurity phase.

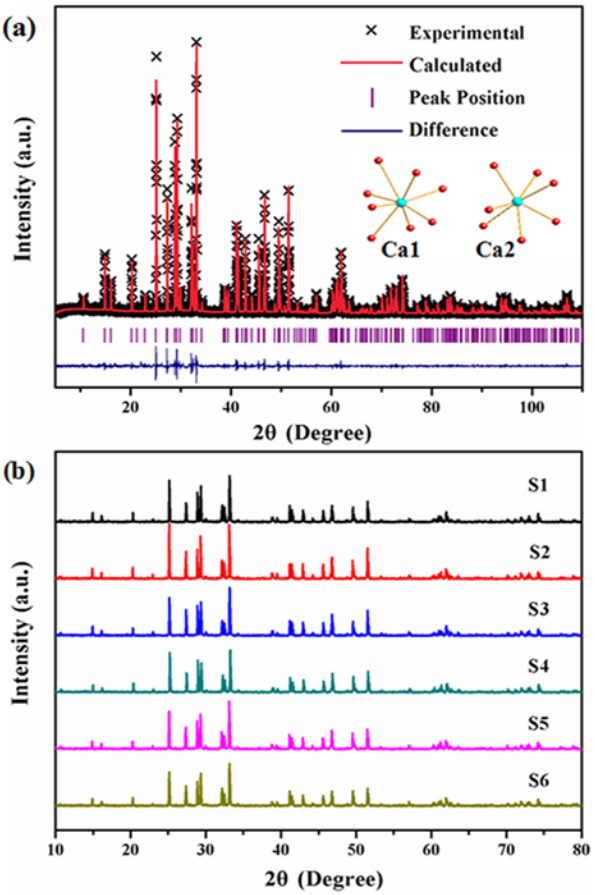


Fig. 1 (a) XRD refinement of $Ca_6BaP_4O_{17}$ host; (b) XRD patterns of $Ca_6BaP_4O_{17}$:0.02$Eu^{2+}$,$yHo^{3+}$ ($0 \le y \le 0.03$).

### 3.2. Band structure

The density functional theory calculations of $Ca_6BaP_4O_{17}$ based on crystal structure refinement are shown in Fig. 2. The local density approximation (LDA) was chosen for the theoretical basis of the density function. This compound possesses a direct bandgap of about 4.081 eV with the valence band (VB) maximum and the conduction band (CB) minimum at the G point of the Brillouin zone. It is expected that the value of the calculated bandgap of about 4.081 eV is smaller than the experimental one as the LDA underestimates the size of the bandgap.[25] The electronic structure of the VB originates predominantly from O 2p states, whereas the CB is composed mostly of Ca 3d states and a small amount of Ba 5d states. $Eu^{2+}$ and $Ho^{3+}$ ions, which occupy $Ca^{2+}$ sites, exchange electrons more easily, resulting in a CB composed of Ca 3d states. With such a large band gap, it is expected that the energy levels of the 5d-4f transitions of the $Eu^{2+}$ ions in the host lattice of $Ca_6BaP_4O_{17}$ should have small interferences with the valence and conduction bands.[26] Thus, $Ca_6BaP_4O_{17}$ host provides a suitable band gap for $Eu^{2+}$ to act as emission center and for $Ho^{3+}$ to act as trap center.

Cite this: DOI: 10.1039/c0xx00000x

www.rsc.org/xxxxxx

ARTICLE TYPE

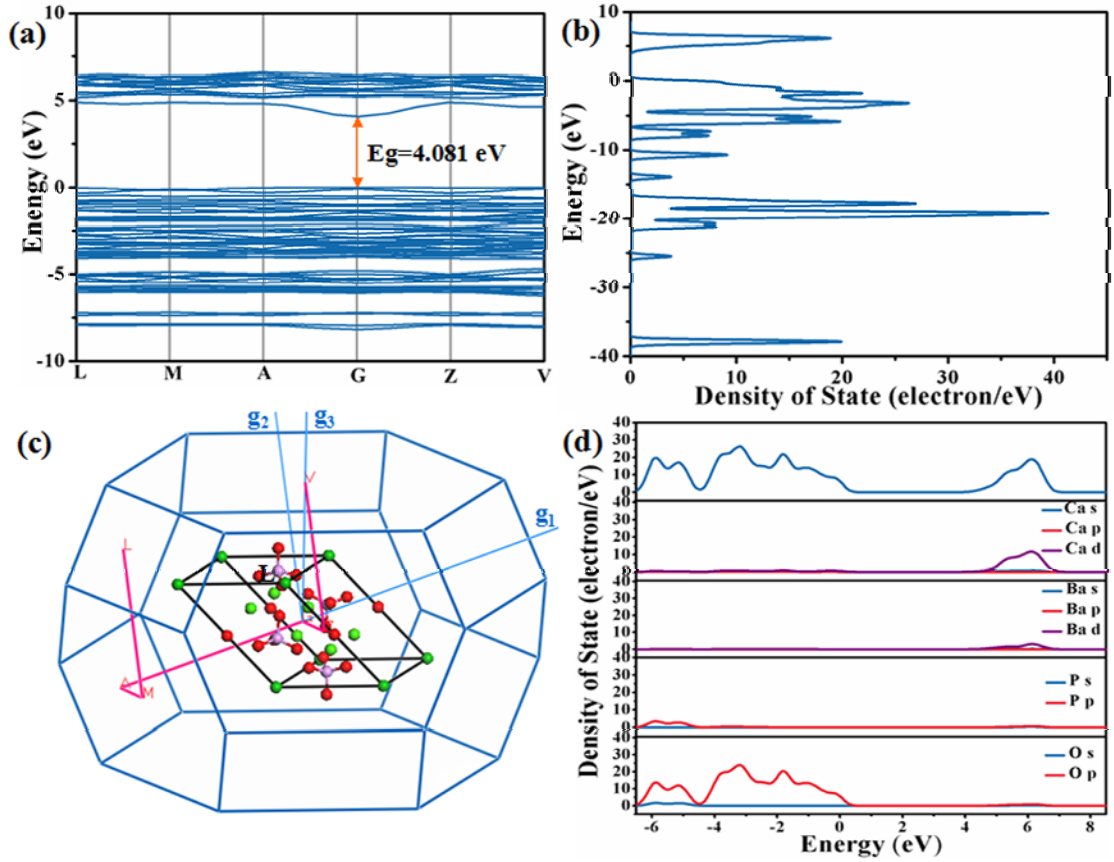


Fig. 2 (a) Band structure; (b) density of states; (c) Brillouin zone; (d) total and partial density of states.

### 3.3. Photoluminescence and phosphorescence properties of $Eu^{2+}$ and $Ho^{3+}$ ions co-doped $Ca_6BaP_4O_{13}$

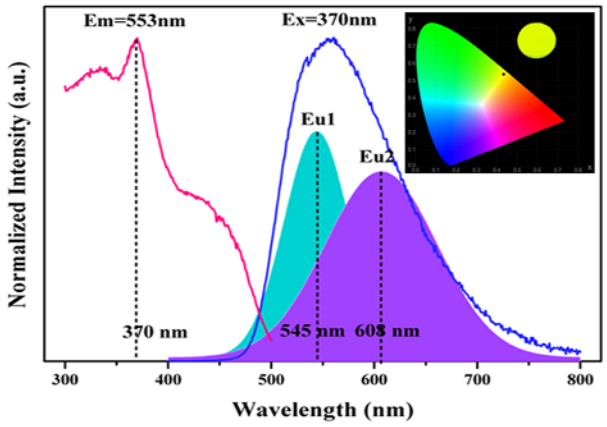


Fig. 3 Excitation and emission spectra of $Ca_6BaP_4O_{17}$:0.02$Eu^{2+}$,0.015$Ho^{3+}$. Inset: CIE chromaticity diagram for $Ca_6BaP_4O_{17}$:0.02$Eu^{2+}$,0.015$Ho^{3+}$ phosphor excited at 370 nm.

As a usual sample, Fig. 3 exhibits normalized excitation and emission spectra for $Ca_6BaP_4O_{17}$:0.02$Eu^{2+}$,0.015$Ho^{3+}$ phosphor at room temperature respectively. Under excitation at 370 nm, the material exhibits only one asymmetric broad band peaking at 553 nm mainly due to the 5d-4f electronic dipole-allowed transition of $Eu^{2+}$ ions. As mentioned in the crystal structure of $Ca_6BaP_4O_{17}$, there are two crystallographically nonequivalent $Ca^{2+}$ sites which can be substituted by the $Eu^{2+}$ ions to produce two nonequivalent emission centers of $Eu^{2+}$ ions in $Ca_6BaP_4O_{17}$. Although the 4f electrons of $Eu^{2+}$ ions are not sensitive to their surroundings, the 5d electrons are split by the crystal field.[27] When crystal field is weak, the emission band of $Eu^{2+}$ ions trends to the short wavelength.[28] Thus, the asymmetric emission of $Ca_6BaP_4O_{17}$:0.02$Eu^{2+}$,0.015$Ho^{3+}$ was well fitted by two Gaussian profiles. We deduce that Eu1 should emit 545 nm light and Eu2 will have a wavelength of 608 nm. A higher emission intensity of Eu1 than Eu2 illustrates that $Eu^{2+}$ ions prefer to occupy Ca1 sites. The excitation spectrum of $Eu^{2+}$ and $Ho^{3+}$ ions co-doped $Ca_6BaP_4O_{17}$ is a broadband from 300 to 500 nm which are mainly ascribed to the allowed transition of $Eu^{2+}$ ions from the 4f ground state to the 5d excited state and partly overlaps the solar irradiation having potential applications in solar energy utilization. Calculated from emission spectra using chromaticity coordinate calculation method based on the CIE1931

(Commission International de I'Eclairage France) system, the CIE chromaticity coordinate of $Ca_6BaP_4O_{17}$:0.02$Eu^{2+}$,0.015$Ho^{3+}$ is (0.43, 0.54) and the color is yellow showed in the inset of Fig. 3.

As shown in Fig. 4, with the concentration of $Ho^{3+}$ ions increasing, no characteristic emissions of $Ho^{3+}$ ions are observed. Clearly, the $Ho^{3+}$ ions are not luminescent centers in this phosphor, but its codoping have great influence on the PL intensity of the phosphor. When the content of $Ho^{3+}$ ions raised to 0.015 mol, its codoping markedly enhanced the PL intensity of the phosphor which could be involved with $Eu^{2+}$ ions redistribution, the defects and lattice distortion of the crystal caused by $Ho^{3+}$ codoping.[29] Besides, the dash curves of Fig. 4 show the phosphorescence spectra of $Ca_6BaP_4O_{17}$:0.02$Eu^{2+}$,0.015$Ho^{3+}$ at different times after the removal of the excitation source. The profiles of the phosphorescence spectra do not change with decay time compared with the emission spectra of $Ca_6BaP_4O_{17}$:0.02$Eu^{2+}$,$y$$Ho^{3+}$ ($0\leq y\leq 0.03$) indicating that the phosphorescence should be derived from the 5d-4f transition of $Eu^{2+}$ ions in the above-mentioned two crystallographic Ca sites rather than $Ho^{3+}$ ions during the afterglow process. In a word, $Eu^{2+}$ ions act as an emission center and $Ho^{3+}$ ions act as a trap center in the co-doped samples.

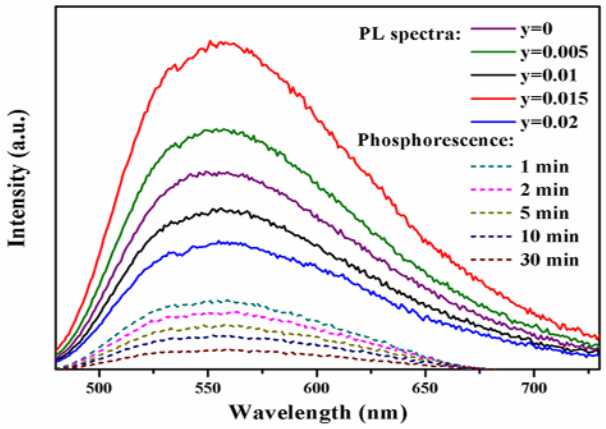


Fig. 4 Emission spectra of $Ca_6BaP_4O_{17}$:0.02$Eu^{2+}$,$y$$Ho^{3+}$ ($0\leq y\leq 0.02$) and phosphorescence spectra of f $Ca_6BaP_4O_{17}$:0.02$Eu^{2+}$,0.015$Ho^{3+}$.

### 3.4. Afterglow decay curves of $Ca_6BaP_4O_{17}$:0.02$Eu^{2+}$,$y$$Ho^{3+}$ ($0\leq y\leq 0.03$)

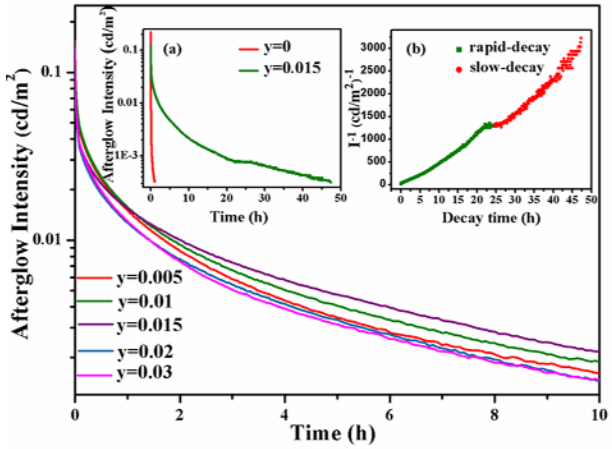


Fig. 5 Afterglow decay curves of $Ca_6BaP_4O_{17}$:0.02$Eu^{2+}$,$y$$Ho^{3+}$ ($0.05\leq y\leq 0.03$). Inset: (a)Afterglow decay curves of $Ca_6BaP_4O_{17}$:0.02$Eu^{2+}$ and $Ca_6BaP_4O_{17}$:0.02$Eu^{2+}$,0.015$Ho^{3+}$; (b)Function of reciprocal afterglow intensity ($I^{-1}$) versus time ($t$) of $Ca_6BaP_4O_{17}$:0.02$Eu^{2+}$,0.015$Ho^{3+}$ excited for 15 min.

To study the decay performance of $Ca_6BaP_4O_{17}$:0.02$Eu^{2+}$,$y$$Ho^{3+}$ ($0\leq y\leq 0.03$) emission in more particulars, the afterglow decay curves for all as synthesized samples (S1-S6) were measured, as shown in Fig. 5. Generally, the afterglow decay process consists of a rapid decay process in the beginning dominating the initial intensity and later a slow decay process responsible for the long-term behavior.[30,31,32,33] Here the decay curves of samples (S1-S6) have been analyzed by curve fitting technique and found that they can be well fitted with a double-exponential equation Eq. (1) as follows:

$$I = A_1 \exp\left(\frac{-t}{\tau_1}\right) + A_2 \exp\left(\frac{-t}{\tau_2}\right) + A_0 \qquad (1)$$

where $I$ and $A_0$ represents the phosphorescence intensity; $A_1$ and $A_2$ are constants; $t$ is the time, and $\tau_1$ and $\tau_2$ are decay time for exponential components, respectively. Since the performance of LLP is chiefly determined by $\tau_2$,[34] the $\tau_2$ of all samples are listed in Table 1. It can be seen that the value of $\tau_2$ increase in the beginning and then decrease later along with the content increase of $Ho^{3+}$ ions. They reach the maximum when the content of $Ho^{3+}$ ions raised to 0.015 mol. Hence, it is suggested that the concentration of $Ho^{3+}$ ions in $Ca_6BaP_4O_{17}$:0.02$Eu^{2+}$ phosphors has great effect on the LLP properties and $Ca_6BaP_4O_{17}$:0.02$Eu^{2+}$,0.015$Ho^{3+}$ sample presents the best LLP characteristic for possessing the longest decay time $\tau_2$. As shown in the left inset of Fig. 5, the initial LLP intensity of $Ca_6BaP_4O_{17}$:0.02$Eu^{2+}$,0.015$Ho^{3+}$ can reach about 0.13 cd/m $^2$ and its LLP can last more than 47 h above the recognizable intensity level (0.32 mcd/m $^2$). Whereas, the phosphorescence of $Ca_6BaP_4O_{17}$:0.02$Eu^{2+}$ can only be visible for 1 h by naked eyes, leading to the afterglow decay curve resembling a vertical line. That phenomenon indicates the phosphorescence of $Ca_6BaP_4O_{17}$:0.02$Eu^{2+}$ is improved largely by the introduction of $Ho^{3+}$ ions and detailed reasons will be discussed later. The afterglow decay curve of $Ca_6BaP_4O_{17}$:0.02$Eu^{2+}$,0.015$Ho^{3+}$ was also plotted as a function of reciprocal persistent luminescence intensity ($I^{-1}$) versus time ($t$), as shown in the right inset of Fig. 5. The $I^{-1} \sim t$ curve was divided into two parts. The two linear

dependence of $I^1$ versus $t$ indicate that long lasting persistent luminescence in the $Ca_6BaP_4O_{17}$:0.02$Eu^{2+}$,0.015$Ho^{3+}$ phosphor is probably caused by two effective trap centers, which will be discussed in the mechanism.

**Table 1** Decay times for two exponential components of $Ca_6BaP_4O_{17}$:0.02$Eu^{2+}$,$yHo^{3+}$ ($0 \le y \le 0.03$)

| Sample no. | $A_0$ | $A_1$ | $\tau_1$ / s | $A_2$ | $\tau_2$ / s |
|---|---|---|---|---|---|
| S1 | 0.0016 | 0.1991 | 5.5336 | 0.0432 | 54.9999 |
| S2 | 0.0017 | 0.0784 | 78.9404 | 0.0467 | 2573.0443 |
| S3 | 0.0017 | 0.0630 | 99.3610 | 0.0463 | 2834.2989 |
| S4 | 0.0015 | 0.0546 | 87.4473 | 0.0358 | 3923.0419 |
| S5 | 0.0017 | 0.0737 | 63.0186 | 0.0387 | 2558.8203 |
| S6 | 0.0016 | 0.0640 | 72.5315 | 0.0398 | 2426.7347 |

### 3.5. TL curves of $Ca_6BaP_4O_{17}$:0.02$Eu^{2+}$,$yHo^{3+}$ ($0 \le y \le 0.03$)

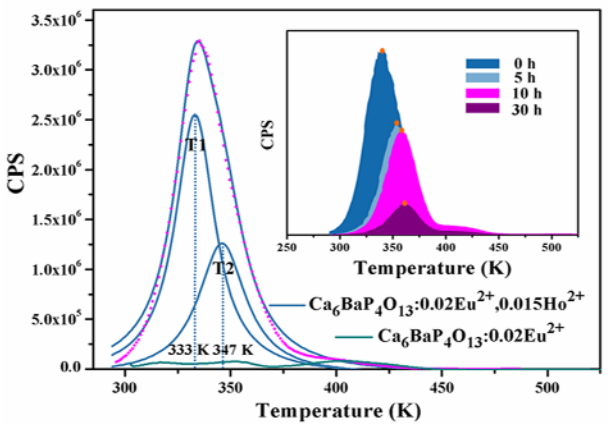


Fig. 6 TL curves of $Ca_6BaP_4O_{17}$:0.02$Eu^{2+}$,0.015$Ho^{3+}$ excited for 2 min. Inset: TL curves of $Ca_6BaP_4O_{17}$:0.02$Eu^{2+}$,0.015$Ho^{3+}$ excited for 2 min and placed in dark room for different times.

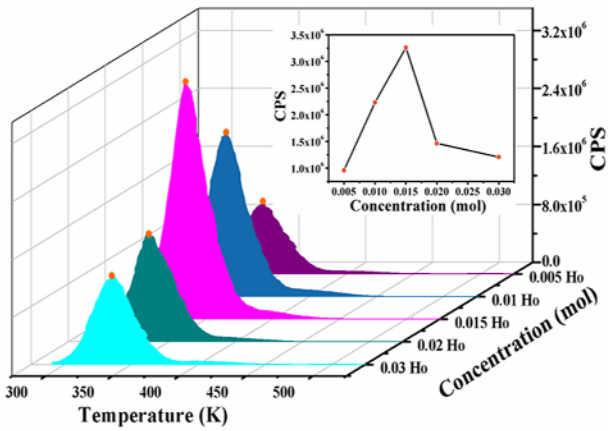


Fig. 7 TL curves of $Ca_6BaP_4O_{17}$:0.02$Eu^{2+}$,$yHo^{3+}$ ($0 \le y \le 0.03$) excited for 2 min.

Trapping centers play a crucial role in the photo-energy storage of persistent and thermo-stimulated phosphors.[35] After the source of excitation is removed, the captured charge carriers can escape under thermal disturbance and transfer to luminescent centers, resulting in phosphorescence. Generally, it is not beneficial for those traps with shallow depths to stabilize the charge carriers, which results in an extremely short period of persistent luminescence duration. Reversely, the charge carriers that are captured by traps with deep depths are very difficult to be released at room temperature leading to poor persistent luminescence performance. So the formation of appropriate trap depth is crucial for achieving LLP performance. Meanwhile, the trap density is also an important influencing factor for LLP. In order to characterize the traps in our samples, TL measurements were performed on $Ca_6BaP_4O_{17}$:0.02$Eu^{2+}$ and $Ca_6BaP_4O_{17}$:0.02$Eu^{2+}$,0.015$Ho^{3+}$ and their TL curves are illustrated in Fig. 6. For $Ca_6BaP_4O_{17}$:0.02$Eu^{2+}$, we just observe three very weak peaks. The TL band is possibly due to intrinsic defects of the host because $Eu^{2+}$ ions equivalently substitute for $Ca^{2+}$ ions in $Ca_6BaP_4O_{17}$:0.02$Eu^{2+}$. Furthermore, the weak TL signal suggests that the concentration of carriers captured at the intrinsic defects is very low.[36] When $Ho^{3+}$ ions are doped, the intensity of one peak is greatly enhanced, and the main peak position moves to 335 K, which means the doping of $Ho^{3+}$ ions largely improves the defect levels. The main peak of $Ca_6BaP_4O_{17}$:0.02$Eu^{2+}$,0.015$Ho^{3+}$ TL curve can be fitted into two Gaussian component located at 333 K and 347 K , respectively. With the careful comparison between $Ca_6BaP_4O_{17}$:0.02$Eu^{2+}$ and $Ca_6BaP_4O_{17}$:0.02$Eu^{2+}$,0.015$Ho^{3+}$ glow curves in Fig. 6, we suppose that there exist new defects in the sample of $Ca_6BaP_4O_{17}$:0.02$Eu^{2+}$,0.015$Ho^{3+}$. The effective TL peak is situated slightly above room temperature (320–400 K), which is a temperature leading to better LLP properties.[37,38] So, in our present work, the TL peaks at 333 K (T1) and 347 K (T2) account for the LLP in room temperature. In order to further estimate the trap state, the trap depths ($E_t$) and trap densities ($n_0$) can be calculated based on the following two Eqs. (2) and (3).[39]

$$E_t = \left[2.52 + 10.2 \times \left(\mu_g - 0.42\right)\right] \times \left(k_B T_m^2\right) / \omega - 2k_B T_m \quad (2)$$

$$n_0 = \omega I_m / \left\{\beta \times \left[2.52 + 10.2 \times \left(\mu_g - 0.42\right)\right]\right\} \quad (3)$$

Where $T_m$ is the temperature of the TL peak, $K_B$ is the Boltzmann constant ($1.38\times10^{-23}$ J $K^{-1}$), $\omega$ is known as the shape parameter and defined as $\omega = \tau+\delta$, $\tau$ is the low-temperature half-width, $\delta$ is the high-temperature half-width, the asymmetry parameter $\mu_g = \delta/(\tau+\delta)$, $\beta$ is the heating rate, and $I_m$ is the intensity of the TL peak. The calculated results $E_t$ and $n_0$ corresponding to band 1 and 2 are presented in Table 2. The former peak (333 K) which has a higher trap density ($3.56\times10^7$) and a low trap depth (0.627 eV) will result in an intense LLP intensity and a relatively rapid decay, while the latter with a lower trap density ($1.69\times10^7$) and a deeper trap depth (0.714 eV) will lead to a long slow one, which correspond to the second order decay process of LLP shown in Fig. 5.

**Table 2** The parameters of the TL curves of $Ca_6BaP_4O_{17}$:0.02$Eu^{2+}$,0.015$Ho^{3+}$.

| Trap | $T_m$ | $\tau$ | $\delta$ | $\omega$ | $\mu_g$ | $E_t$ | $n_0$ |
|---|---|---|---|---|---|---|---|
| 1 | 333 | 20 | 14 | 34 | 0.412 | 0.627 | $3.56\times10^7$ |
| 2 | 347 | 17 | 10 | 27 | 0.370 | 0.714 | $1.69\times10^7$ |

In order to investigate the number of trapping centers concerned and the kinetic order of the TL, the TL glow curves of sample $Ca_6BaP_4O_{17}$:0.02$Eu^{2+}$,0.015$Ho^{3+}$ with different delay time were recorded in the inset of Fig. 6. The results suggest that the TL intensity of the glow peak reduces and the peak position of the glow curve gradually shifts to higher temperature. According to the research of Wu *et al*.[40], two possibilities could be responsible for the shifting TL peak maximum. One possibility is that many traps of closer depth comprise a trapping center, leading to a broad TL spectrum, in which case, the lower temperature ingredients will decay relatively faster than the higher temperature ones so justifying the TL peak to shift. The full width at half maximum ($\omega$) of TL curve will diminish as the delay time increases. From the results listed in Table 3, we can see the full width at half maximum to become gradually diminished with increased delay time, suggesting the model containing closely spaced traps with varying depths is applicable. We also recorded the TL spectra of samples S2-S6 in Fig.7. All samples were measured after exposure to UV-irradiation 2 min. The TL spectra of samples show intensity increases until the $Ho^{3+}$ ions concentration reaches 0.015 mol before decreasing as concentration quenching occurs. Due to the nonequivalent substitution, an excess of positive charge in the host must be compensated. The only possible way to fulfill the charge compensation is that two $Ho^{3+}$ ions replace three $Ca^{2+}$ ions to balance the charge of the phosphor, which will create two $Ho_{Ca}^{\cdot}$ positive defects and one $V_{Ca}''$ negative defect. Therefore, the doped $Ho^{3+}$ ions concentrations greatly affect trap density. The trap centers increase with the increasing content of $Ho^{3+}$ ions up to 0.015 mol, then decrease beyond the content. A higher trap concentration means more free excited electrons are captured by electron-traps rather than immediately to emission centers leading to darker initial phosphorescence and longer afterglow duration. For this reason, Sample S4 shows the best afterglow performance for the greatest value of trap density, which is consistent with the result of the decay curve analysis.

**Table 3** The parameters of the TL curves of sample S4 with different delay time.

| Delay time | *Tm*/K | $\omega$/K | $\mu_g$ |
|---|---|---|---|
| 0 h | 340 | 40 | 0.525 |
| 5 h | 354 | 34 | 0.5 |
| 10 h | 358 | 33 | 0.515 |
| 30 h | 361 | 32 | 0.5 |

### 3.6 Afterglow mechanism of $Eu^{2+}$ and $Ho^{3+}$ ions co-doped $Ca_6BaP_4O_{13}$

The above results clearly show that $Ca_6BaP_4O_{17}$:0.02$Eu^{2+}$,$y$$Ho^{3+}$ ($0\leq y\leq 0.03$) has excellent persistent luminescence. $Eu^{2+}$ ions which occupy Ca1 and Ca2 sites acts as an emission center and $Ho^{3+}$ ions which occupy Ca1 site acts as a trap center in the co-doped samples. So the introduction of $Ho^{3+}$ ions into $Ca_6BaP_4O_{13}$ matrix can be accomplished via the following pathway:

$$\left[2Ho^{3+}+3Ca^{2+}\rightarrow 2Ho^{3+}{}_{Ca^{2+}}^{\bullet}+V_{Ca^{2+}}''\right] \quad (4)$$

which creates two positive defects $Ho_{Ca}^{\cdot}$ and one negative defect $V_{Ca}''$ to get the charge compensation. All of the experiments indicate that there exist highly efficient trapping levels in this material. A possible afterglow mechanism for the formation of such an efficient yellow emission long-persistent phosphor of $Eu^{2+}$ and $Ho^{3+}$ ions co-doped $Ca_6BaP_4O_{17}$ is exhibited in Fig. 8. $Eu^{2+}$ ions have been recognized as an excellent activator for long-persistent phosphors because its 5d electron state is usually close to the CB of the host, which makes trapping of electrons possible.[41] After UV-light excitation, electrons in the valence band (VB) are excited directly through the host into the conduction band (CB) (process 1). Some of excited electrons can shift freely in the CB and transfer to $4f^65d^1$ level of $Eu^{2+}$ ions, whereas the holes left behind move randomly in the VB. Then electron transitions occur from the $4f^65d^1$ level to lower levels $4f^7$ followed by the characteristic emissions of $Eu^{2+}$ ions as luminescence (process 2). After switching off the ultraviolet light source, the residual electrons moving in the CB can be trapped by $Ho_{Ca}^{\cdot}$ whereas holes shifting in VB can be trapped by $V_{Ca}''$ instead of returning to the ground state (process 3). Under thermal agitation, the carriers (electrons and holes) will be released from the trapping centers and transfer via the host to the $Eu^{2+}$ ions after a series of non-radiation transitions (process 4), followed by recombination and causing the characteristic emissions of $Eu^{2+}$ ions as persistent phosphorescence (process 5). The whole process is consistent with the generally accepted mechanism that persistent luminescence occurs through the direct recombination of the conduction electrons released from traps with the emission centers.

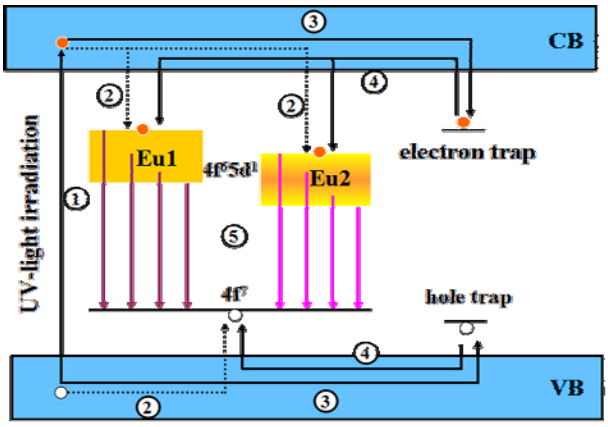


Fig.8. The schematic diagram of phosphorescence mechanism for ($Ca_6BaP_4O_{17}$:0.02$Eu^{2+}$,$y$$Ho^{3+}$ ($0\leq y\leq 0.03$).

## 4. Conclusions

In summary, a novel yellow emitting long-persistent phosphor $Ca_6BaP_4O_{17}$:0.02$Eu^{2+}$,0.015$Ho^{3+}$ with excellent afterglow properties was successfully identified via a high temperature solid state method. $Eu^{2+}$ ions show a broad asymmetric emission band located at 553 nm, because of the two different $Ca^{2+}$ sites in $Ca_6BaP_4O_{17}$. The influence of $Ho^{3+}$ ions concentrations on PL, afterglow decay curves and TL properties were studied revealing the double exponential decay mode in $Ca_6BaP_4O_{17}$:$Eu^{2+}$,$Ho^{3+}$ phosphor. At least two types of independent traps corresponding to peaks at about 333 K and 347 K exist in

$Ca_6BaP_4O_{17}$:0.02$Eu^{2+}$,0.015$Ho^{3+}$ material and all of them responsible for the visible long lasting phosphorescence. According to analysis of TL glow curves, the defects $V_{Ca}$" were regarded as hole traps, while the defects $Ho_{Ca}^{\cdot}$ were regarded as electron traps. The result indicted that suitable trap depth and high trap concentration are critical to the energy storage and excellent performance of LLP and new traps caused by $Ho^{3+}$ ions have an indelible effect on its afterglow. A possible afterglow mechanism is proposed and the processes of LLP are explained. This brand new LLP material exhibiting a 47 h afterglow will have great potential to be applied commercially in many different fields.

## Acknowledgments

This work was supported by Specialized Research Fund for the Doctoral Program of Higher Education (No. 20120211130003) 35 and the National Natural Science Funds of China (Grant No. 51372105).

## Notes and references

*Department of Materials Science, School of Physical Science and Technology, Lanzhou University, Lanzhou, 730000, PR China and Key Laboratory for Special Function Materials and Structural Design of the Ministry of Education, Lanzhou University, Lanzhou 730000, China.*
**Corresponding author: Yuhua Wang*
*Email address: wyh@lzu.edu.cn; tel.: +86 931 8912772; fax: +86 931 8913554.*

1. M. Allix, S. Chenu, E.Véron, T. Poumeyrol, E. A. Kouadri-Boudjelthia, S. Alahrache, F. Porcher, D. Massiot and F. Fayon, *Chem. Mater.*, 2013, **25**, 1600-1606.
2. J. Wang, Q. Su and S. B. Wang, J. Phys. *Chem. Solids.*, 2005, **66**, 1171-1176.
3. E. Pavel, I. N. Mihailescu, A. Hening and V. I. Vlad, *Opt. Lett.*, 1998, **23**, 1304-1306.
4. H. H. Li, S. Yin, Y. H. Wang and T. Sato, *Appl. Catal. B.*, 2013, **132-133**, 487-492.
5. B. Wang, H. Lin, Y. L. Yu, D. Q. Chen, R. Zhang, J. Xu and Y. S. Wang, *J.Am.Ceram.Soc.*, 2014, **97**, 2539-2545.
6. T. Matsuzawa, Y. Aoki, N. Takeuchi and Y. Murayama, *J. Electrochem. Soc.*, 1996, **143**, 2670-2673.
7. B. Qu, B. Zhang, L. Wang, R. Zhou and X. C. Zeng, *Chem. Mater.*, 2015.
8. R. Chen, Y. Wang, Y. Hu, Z. Hu and C. Liu, *J. Lumin.*, 2008, **128**, 1180-1184.
9. J. Niittykoski, T. Aitasalo, J. Hölsä, H. Jungner, M. Lastusaari, M. Parkkinen and M. Tukia, *J. Alloys Compd.*, 2004, **374**, 108-111.
10. Z. Qiu, Y. Zhou, M. Lü, A. Zhang and Q. Ma, *Acta Mater.*, 2007, **55**, 2615-2620.
11. Y. Lin, Z. Tang, Z. Zhang, X. Wang and J. Zhang, *J. Mater. Sci. Lett.*, 2001, **20**, 1505-1506.
12. Y. Lin, Z. Tang and Z. Zhang, *Mater. Lett.*, 2001, **51**, 14-18.
13. F. Clabau, X. Rocquefelte, S. Jobic, P. Deniard, M. H. Whangbo, A. Garcia and T. Le Mercier, *Chem. Mater.*, 2005, **17**, 3904-3912.
14. X. Y. Sun, J. H. Zhang, X. Zhang, Y. S. Luo and X. J.Wang, *J. Phys. D: Appl. Phys.*, 2008, **41**, 195414 (4pp).
15. Z. Hong, P. Zhang, X. Fan and M. Wang, *J. Lumin.*, 2007, **124**, 127-132.
16. VK. Van den Eeckhout, P. F. Smet and D. Poelman, *J. Lumin.*, 2009, **129**, 1140-1143.
17. L. Lin, M. Yin, C. Shi and W. Zhang, *J. Alloys Compd.*, 2008, **455**, 327-330.
18. J. Hölsä, *Electrochem. Soc. Interface.*, 2009, **18**, 42-45.
19. Y. S. Tang, S. F. Hu, C. C. Lin, N. C. Bagkar and R. S. Liu, *Appl. Phys. Lett.*, 2007, **90**, 108-151.
20. N. Komuro, M. Mikami, Y. Shimomura, E. Bithell and A. K. Cheetham, *J. Mater. Chem. C.*, 2014, **2**, 6084-6089.
21. N. Komuro, M. Mikami, Y. Shimomura, E. Bithell and A. K. Cheetham, *J. Mater. Chem. C.*, 2015, **3**, 204-210.
22. P. Dorenbos, *J. Phys.: Condens. Matter.*, 2003, **15**, 8417.
23. H. Rietveld, *Acta Crystallogr*, 1967, **22**, 151-152.
24. H. Rietveld, *J. Appl. Crystallogr.*, 1969, **2**, 65-71.
25. Y. Q. Li, Y. H. Wang, X. H. Xu, G. Yu and F. Zhang, *J. Electrochem. Soc.*, 2010, **157**, J39-J43.
26. Y. Li, Y. Fang, N. Hirosaki, R. Xie, L. Liu, T. Takeda and X. Li, *Materials*, 2010, **3**, 1692.
27. P. Wang, X. Xu, D. Zhou, X. Yu and J. Qiu, *Inorganic chemistry*, 2015, **54**, 1690-1697.
28. Y. Gong, Y. Wang, Y. Li, X. Xu and W. Zeng, *Optics express*, 2011, **19**, 4310-4315.
29. D. Zhong, X. Y. Hu, Z. H. Li and Y. X. Li, *J. Chin. Soc. Rare Earths.*, 2009, **27**, 36.
30. J. Zhang, X. Ma, Q. Qin, L. Shi, J. Sun, M. Zhou, B. Liu and Y. Wang, *Mater. Chem. Phys.*, 2012, **136**, 320-324.
31. J. Wang, S. Wang and Q. Su, *J. Mater. Chem.*, 2004, **14**, 2569-2574.
32. R. Pang, C. Li, L. Shi and Q. Su, *J. Phys. Chem. Solids.*, 2009, **70**, 303-306.
33. B. Lei, H. Zhang, W. Mai, S. Yue, Y. Liu and S. Man, *Solid State Sci.*, 2011, **13**, 525-528.
34. T. Wang, Y. H. Hu, L. Chen, X. J. Wang and G. F. Ju, *Radiation Measurements*, 2015, **73**, 7-13.
35. D. Jia, W. Jia, D. Evans, W. Dennis, H. Liu, J. Zhu and W. Yen, *J. Appl. Phys.*, 2000, **88**, 3402-3407.
36. T. Matsuzawa, Y. Aoki, N. Takeuchi and Y. Murayama, *J. Electrochem. Soc.*, 1996, **143**, 2670-2673.
37. X. Sun, J. Zhang, X. Zhang, Y. Luo and X. J. Wang, *J. Phys. D:Appl. Phys.*, 2008, **41**, 195414.
38. Y. Liu, B. Lei and C. Shi, *Chem. Mater.*, 2004, **17**, 2108-2113.
39. R. Chen, *J. Appl. Phys.*, 1969, **40**, 570-585.
40. H. Wu, Y. Hu and X. Wang, *Radiat. Meas.*, 2011, **46**, 591-594.
41. F. Clabau, X. Rocquefelte, T. Le Mercier, P. Deniard, S. Jobic and M. H. Whangbo, *Chem. Mater.*, 2006, **18**, 3212-3220.

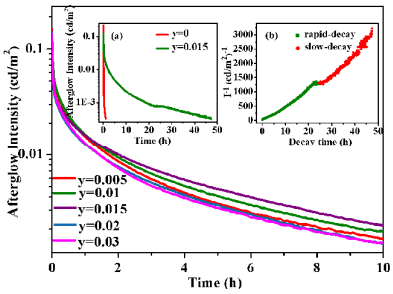


The brand new LLP material $Ca_6BaP_4O_{17}:Eu^{2+},Ho^{3+}$ exhibites about 0.13 cd/m $^2$ initial LLP intensity and a 47 h afterglow.